文章编号：1001－9014(2015)05－0538－07

DOI:10.11972/j.issn.1001－9014.2015.05.005

# Intersubband optical absorptions of a GaN-based step quantum well with built-in electric field

ZHANG Li

(Institute of Electronic Technique and Material Development, Guangzhou Panyu Polytechnic, Guangzhou 511483, China)

**Abstract**: By using the compact density matrix approach, the linear and nonlinear optical absorption coefficients in a GaN-based step quantum well (QW) with strong built-in electric field (BEF) have been theoretically deduced and investigated in detail. The band nonparabolicity is taken into account by using an energy-dependent effective mass (EDEM) method. The exact electronic eigen-states in the step QW with strong BEF were obtained and the simple analytical formulas for the linear and nonlinear optical absorption coefficients in the systems were also deduced. Numerical calculations on an AlN/GaN/$Al_xGa_{1-x}N$/AlN step QW were performed. It is found that the decreasing of well width $L_w$ and step barrier width $L_b$ and the doped concentration x in step barrier can result in the enhancement of the absorption coefficients. Moreover, with the decrease of $L_w$, $L_b$ and x, the photon energies of absorption have blue-shift, and the full-width-at-half-maximum of the total absorption coefficient increases and the saturation absorption intensity decrease. Some results are consistent with recent experimental observations.

**Key words**: density matrix approach, absorption coefficient, built-in electric field

**PACS**: 78.66.Fd, 42.65.Ky, 42.79.Nv

# 有强内电场的 GaN-基阶梯量子阱中的线性与非线性光吸收

张　立

(广州番禺职业技术学院 电子技术与材料开发研究所,广东 广州　511483)

**摘要**:采用密度矩阵方法,考察了带强内建电场 GaN-基阶梯量子阱中的线性与非线性光吸收系数.基于能量依赖的有效质量方法,在考虑了带的非抛物性情况下,推导了结构中的精确解析的电子本征态,给出了系统中简单解析的线性与非线性光吸收系数表达式.以 AlN/GaN/$Al_xGa_{1-x}N$/AlN 阶梯量子阱为例进行了数值计算.结果发现阶梯量子阱的阱宽 $L_w$、阶梯垒宽 $L_b$、阶梯垒的掺杂浓度 $x$ 的减小将提高体系的吸收系数.而且,随着 $L_w$,$L_b$ 和 $x$ 减小,吸收光子的能量有明显的蓝移,总吸收系数的半宽度及饱和吸收强度均减小.计算获得的部分结果与最近的实验观察完全一致.

**关　键　词**:密度矩阵方法;吸收系数;内电场

**中图分类号**:O431.2　　**文献标识码**:A

## Introduction

Optical absorption is one type of important physical phenomenon and interaction which usually occurs between light and matter. After the laser was invented, not only the linear optical absorption, but also the nonlinear optical absorption can be observed in experiments. The study of linear and nonlinear optical absorptions in low-dimensional quantum systems is essential for developing semiconductor quantum micro-devices and is helpful for understanding the carrier dynamics processes such as electron relaxation. After knowing the physical essence of optical absorption, researchers focus their attentions on finding ideal quantum material and suitable quantum confined structures for realizing desired linear and non-

**Received date**: 2014 - 07 - 04, **revised date**: 2014 - 09 - 03　　**收稿日期**:2014 - 07 - 04, **修回日期**:2014 - 09 - 03

**Foundation items**:This work was jointly supported by the NNSF of China (60906042 and 61178003), the Yangchen Scholar Project (10B010D) and the STPAA (10B001) of Guangzhou City, STP of Panyu Region (2010-D-09-1103004) and Project of Academic Innovation Group of Guangzhou City (13C17)

**Biography**:Zhang Li (1976-), male, Jinzhou City, Hubei Province, Ph. D. Physical professor. Majoring in optical nonlinearity and electron－phonon interaction in semiconductor nanometer structures.

* **Corresponding author**:E-mail: zhangli-gz@263.net

linear optical absorptions.

Currently, the optical absorption properties of GaN-based quantum heterostructures based on the intersubband (ISB) transitions have attracted much interest both in theoretical and experimental investigations[1-2]. The driving force behind these research efforts is mainly due to the following three evident facts: (1) The nitride materials possess strong atomic bonding and wide bandgap, such as GaN/AlN heterosturcture. Its band offset reaches nearly 2 eV which covers the optical telecommunication wavelengths (~1.55 μm). (2) The ultra fast ISB carrier dynamics (in the order of picosecond and sub picosecond) due to a strong Fröhlich interaction in these highly ionic materials makes them promising candidates for high-speed ISB optical devices such as optical switches operating at Tbit/s data rate[1]. (3) The strong built-in electric field (MV/cm) in the nitride heterostructures originating from the piezoelectric and spontaneous polarizations breaks naturally the inversion symmetry of the confined potential profile for carrier[2-3]. This results in very large even-order optical nonlinear susceptibility and other fancy optical features in the nitride heterostructure systems.

In fact, bearing this ideal in mind, several authors investigated the linear and nonlinear optical properties of GaN-based quantum confined system[1-2,4-9]. For example, Lizuka's group[1] investigated experimentally the ISB optical absorptions in GaN/AlGaN quantum wells (QWs). An ultrashort relaxation time of less than 150 fs was observed, and the saturation energy density of 0.5 pJ/μm$^2$ at a wavelength of 1.46 μm was obtained. Baumann and coworkers reported electromodulated ISB absorption experiments on AlN/GaN superlattices (SLs) grown on a transistor-like structure. It is found that absorption peaks can be adjusted by applying an external field. Tchernycheva and cooperators[2] studies the ISB optical absorption in GaN/AlN double QWs both in theories and experiments, and they found that the band nonparabolicity influences the energy difference as large as 25%. Li and Paiella[4] brought forward a numerical model based on the self-consistent solution of Schrödinger, Poisson and carrier-density rate equations to design GaN/AlGaN coupled QWs optimized for application. Result indicates that the saturation intensity in GaN-based coupled QWs is over 30 times smaller compared with that in uncoupled ones. Malis et al[5] observed directly strong near-infrared ISB absorption at room temperature in InGaN/GaN SLs grown by molecular-beam epitaxy. Monroy et al[6] investigated the influences of polar and semipolar on the infrared absorption spectra in AlGaN/GaN SLs. Hofstetter's team[7] reviewed the near-infrared photodetectors based on ISB transitions in AlN/GaN SLs. They pointed out that such devices can work at frequencies up to tens of GHz, show interesting nonlinear effects, and are capable of integration with transistors or ultraviolet detectors. Naranjo et al[8] studies the nonlinear optical absorption of InN/InGaN SLs operating in the telecommunication regime. An enhancement of nonlinear absorption compared with bulk InN was observed. Recently, Ive et al[9] designed AlN/GaN multiple quantum well structures for intersubband transitions based on effective-mass approximation and Schrödinger-Poisson calculations, and they found that short 1.55 ~ 3.0 μm wavelengths require 0.5 ~ 1.5 nm wide homogeneous barriers with abrupt AlN/GaN heterointerfaces. Furthermore, the investigations of optical absorption were also extended to the GaN-based cylindrical quantum dots (QDs), spherical QDs and truncated pyramids-shaped QDs.

However, to the best of our knowledge, there has been little work to investigate the optical absorption features in GaN/AlGaN step QW structures by now. As stated above, GaN-based step QW is an asymmetrical quantum confined structures, and it possesses more adjustable structural parameters in contrast to the single GaN-based QW. Moreover, there are quite strong built-in electric fields (BEFs, ~MV/cm) in the vicinity of the heterostructures originating from the strong spontaneous macroscopic polarization and large piezoelectric coefficients[14]. Thus GaN-based step QW could display special linear and nonlinear optical properties other than single GaN-based QWs and coupled QWs[1,2]. Hence it is necessary and important to investigate the optical absorption properties in GaN/AlGaN step QWs.

In fact, the linear and nonlinear optical properties in GaAs-based step QW structures have been extensively studied and reported[10-12]. For example, Rosencher and Bois[10] analyzed optical nonlinearities in asymmetric step QWs due to resonant intersubband transitions by using a compact density-matrix approach, and the large dipolar matrix elements were obtained in such structures. Ynh and Wang[11] theoretically studied the field-dependent optical properties of a step QW structure, which consists of a small well inside a big well. Recently, Wang and coworkers[12] investigated the effect of spatial nonlocality on the second harmonic generation and terahertz optical interaction in GaAs/AlGaAs step QWs. These studies reveal that step QWs possess more adjustable parameters and larger dipole matrix element in contrast to the single QW structures. Though the optical nonlinearities of nitride double QWs have been analyzed by the present authors[32], the features of linear and nonlinear optical absorption in wurtzite GaN-based step are not investigated and reported to the best our knowledge. Furthermore, other than the GaAs-based heterostructure, there are quite strong BEF in the GaN-based heterostructure, which may influence greatly the electronic states and optical nonlinearity. These factors motivate us to investigate optical absorption properties in GaN-based step QWs in the present work.

The main accomplishments and significance of this work can be summarized as the following three points. Firstly, taking into account the band nonparabolicity and strong BEF effect, the analytical and exact electronic states in the GaN-based step QWs were derived by using an energy dependent effective mass (EDEM) method and the two Airy functions. Secondly, numerical calculations on an AlN/GaN/AlGaN/AlN step QW were performed. It is found that the decreasing of well width $L_w$ and step barrier width $L_b$ and the doped concentration x in step barrier will result in the enhancement of the absorption coefficients. Thirdly, with the decrease of $L_w$,

$L_b$ and x, the photon energies of absorption have blue-shift, and the full-width- at-half-maximum (FWHM) of the total absorption coefficient increases and the saturation absorption intensity decreases. Some results obtained here are consistent with the recent experiments[6].

The paper is organized as follows: In Sect. 1, by adopting the methods of effective mass and envelope wave-function, the electronic eigen-states in nitride step QWs with strong BEF were exactly solved with the aid of two Airy functions. The band nonparabolicity was taken into account by using a treatment of energy dependence effective mass. Then under the compact density matrix approach, the simple analytical formulas for the linear and nonlinear optical absorption coefficients in the systems were deduced. In Sect. 2, numerical calculations on a typical AlN/GaN/$Al_xGa_{1-x}$N/AlN four-layer step QW structure were performed. The dependences of the linear and nonlinear optical absorption coefficients on the structural parameters (the well width, the barrier width and the doped concentration of the central step barrier) and the saturation absorption intensity were analyzed and discussed.

## 1 Theory

Considering a four-layer wurtzite step QW with the well width and the step barrier width being $L_w$ and $L_b$, respectively ($L_w = z_1$ and $L_b = z_2 - z_1$). We take the z-axis along the direction of the c-axis of the wurtzite material and denote the radial- (axial-) direction as t (z). The three heterostructure interfaces are located at $z = z_0$; $z_1$; $z_2$, respectively (Referring to the Fig. 1). As stating above, there are strong BEF originated from the spontaneous polarization $P_{SP}$ and piezoelectric polarization $P_{PE}$ in the vicinity of the hetero-interfaces of the wurtzite nitride QWs[3]. The direction of the spontaneous polarization is determined by the polarity of the crystal, while the direction of the piezoelectric polarization depends on the polarity and whether the material is under tensile or compressive stress. For simplicity, we ignore the complicated strain of the thick AlN barrier layers due to the lattice and thermal mismatch of the GaN and central AlGaN barrier layers following the treatments of Shi and Takeuchi[3]. In this case, the strength of built-in electric field induced by the piezoelectricity and spontaneous polarization in GaN well layer is given by[3].

$$F^{GaN} = -\frac{(P_{SP}^{GaN} + P_{PE}^{GaN} - P_{SP}^{AlN})}{e_0 e_e^{GaN}} \quad , \quad (1)$$

and the strength of built-in electric field in the central AlGaN barrier layer is read as

$$F^{AlGaN} = -\frac{(P_{SP}^{AlGaN} + P_{PE}^{AlGaN} - P_{SP}^{AlN})}{e_0 e_e^{AlGaN}} \quad , \quad (2)$$

where $P_{SP}^{v}$ and $P_{PE}^{v}$ denote the spontaneous and the piezo-elec-tric polarizations of layer $v$ ($v$ = GaN, AlGaN), $e_e$ is the electronic dielectric constant of material $v$, respectively. The schematic diagram of the potential profile taking into account the BEF is also given in Fig. 1. Under the effective mass and envelope wave-function approximations, the electronic eigen-functions of the step QWs with BEF are expressed by

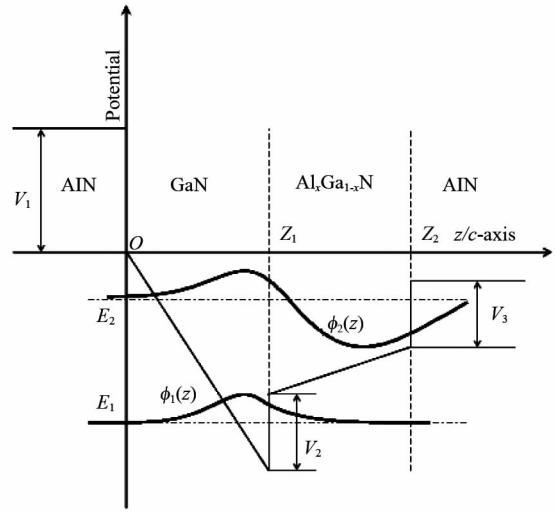


Fig. 1 Schematic diagram of confined potential profile and electronic wave-functions of the ground-state $\phi_1(z)$, and the first-excited state $\phi_2(z)$ in $z$-direction of the wurtzite GaN-based step QW

图1 纤锌矿 GaN-基阶梯量子阱中 $z$-方向上及受限电势剖面图及电子基态 $\phi_1(z)$、第一激发态波函数 $\phi_2(z)$

$$\Phi_{n,k}(\boldsymbol{r}) = \phi_n(z) U_c(\boldsymbol{r}) \exp(i\boldsymbol{k}_{||} \cdot \boldsymbol{r}_{||}) \quad \exp(ik_{||} r_{||}) U_c(\boldsymbol{r})$$
$$\begin{cases} A_1 \exp(k_1 z) & z < -z_0 \\ A_2 \mathrm{Ai}[\xi_2(z)] + B_2 \mathrm{Bi}[\xi_2(z)] & z_0 < z < z_1 \\ A_3 \mathrm{Ai}[\xi_3(z)] + B_3 \mathrm{Bi}[\xi_3(z)] & z_1 < z < z_2 \\ B_4 \exp(-k_4 z) & z > z_2 \end{cases} \quad , \quad (3)$$

where $k_{||}$ and $r_{||}$ are the wave vector and coordinate in the $xy$ plane, $U_c(r)$ is the periodic part of the Bloch function in the conduction band at $k = 0$, and $\mathrm{Ai}(x)$ and $\mathrm{Bi}(x)$ are the two Airy functions. The symbol $k_i$ ($i$ = 1, 4) in Eq. (3) denotes the electronic wave-numbers in the ranges of $[-\infty, -z_0]$ and $[z_2, +\infty]$, respectively, and they are given by

$$k_1 = \sqrt{\frac{2m_{E1}^*(V_1 - E_n)}{\hbar^2}} \quad , \quad (4)$$

and

$$k_4 = \sqrt{\frac{2m_{E4}^*(V_2 + V_3 - eF_1 L_w - eF_2 L_b - E_n)}{\hbar^2}} \quad . \quad (5)$$

The other two functions $\xi_i(z)$ ($i$ = 2, 3) in the Eq. (3) are defined as

$$\xi_2(z) = -\left[\frac{2eF_1 m_{E2}^*}{\hbar^2}\right]^{1/3} \left[\frac{eF_1 z - E_n}{eF_1}\right] \quad , \quad (6)$$

and

$$\xi_3(z) = -\left[\frac{eF_2 m_{E3}^*}{\hbar^2}\right] \left[\frac{V_2 + eF_1 z + eF_2(z - z_1) - E_n}{eF_2}\right] . \quad (7)$$

In Eqs. (4-7), $V_i$ ($i$ = 1, 2, 3) are conduction band offsets at the interfaces (referring to Fig. 1), and $m_{Ei}^*$ ($i$ = 1, 2, 3, 4) is the EDEM of the electron which is usually

employed to describe the band nonparabolicity. Here we take the simple form of EDEM as

$$m_{Ei}^{*} = m_{ei}^{*}\left[\frac{2E_n}{E_g}+1\right] \quad , \quad (8)$$

where $m_{ei}^{*}$ is the electron effective mass at the Γ-point, $E_g$ is the energy gap of the nitride materials, and $E_n$ is the discrete electron eigen-energy in z-direction. The eigen-energy $E_n$ of the step QWs in z-direction can be numerically solved by the standard boundary condition of electronic bound states. The total eigen-energies corresponding to the bound state is given by

$$\varepsilon_{n,k} = E_n + \frac{\hbar^2}{2m^{*}}|\vec{k}_{\parallel}|^2 \quad . \quad (9)$$

Next the formulas of the linear and nonlinear optical absorptions in this step QW model are deduced. Assuming a monochromatic incident field $E(t)=\tilde{E}\exp(-iwt)+\tilde{E}^{*}\exp(iwt)$ is applied to the system. The evolution of the density matrix is given by the time-dependent Schrödinger equation

$$\frac{\partial\rho_{ij}}{\partial t} = \frac{1}{i\hbar}[H_0 - qzE(t),\rho]_{ij} - \Gamma_{ij}(\rho-\rho^{(0)})_{ij} \quad . (10)$$

For simplicity, only one value of the relaxation rate is assumed, namely, $\Gamma_0 = 1/T$. Eq (10) is solved using the usual iterative method[5-8],

$$\rho(t) = \sum_n \rho^{(n)}(t) \quad , (11)$$

with

$$\frac{\partial\rho_{ij}^{(n+1)}}{\partial t} = \frac{1}{i\hbar}\{[H_0,\rho^{n+1}]_{ij} - i\hbar\Gamma_{ij}\rho_{ij}^{(n+1)}\} - \frac{1}{i\hbar}[qz,\rho^{(n)}]_{ij}E(t) \quad . \quad (12)$$

The electronic polarization $P(t)$ and susceptibility $\chi(t)$ caused by the optical field $E(t)$ can be expressed through the dipole operator $M$ and the density matrix as

$$P(t) = \chi_0\varepsilon(w)\tilde{E}e^{-iwt} + \varepsilon_\chi c(-w)\tilde{E}^{*}e^{iwt} = \frac{1}{V}\mathrm{Tr}(rM) \quad , \quad (13)$$

where $V$ and $\rho$ are the volume and the one-electron density matrix of the system, respectively. $\varepsilon_0$ is the permittivity of free space, and the symbol "Tr" denotes the summation over the diagonal elements of the matrix. The susceptibility $c$ is related to the absorption coefficient $\alpha(w)$ by

$$\alpha(w) = w\sqrt{\frac{\delta}{e_R}}\mathrm{Im}[\varepsilon_0\chi(w)] \quad , \quad (14)$$

where $\delta$ is the permeability of the system, $\varepsilon_R$ is the real part of the permittivity, and $\chi(w)$ is the Fourier component of $\chi(t)$ with $\exp(-iwt)$ dependence. By using the same compact-density matrix approach and iterative procedure, the linear and the third-order absorption coefficients $\alpha^{(1)}(w)$ and $\alpha^{(3)}(w)$ are derived, and they are given by

$$\alpha^{(1)}(w) = w\sqrt{\frac{\delta}{\varepsilon_R}}\frac{|\mu_{21}|^2\sigma_v\hbar\Gamma_0}{(E_{21}-\hbar w)^2+(\hbar\Gamma_0)^2} \quad , \quad (15)$$

$$\alpha^{(3)}(w,I) = -w\sqrt{\frac{\delta}{\varepsilon_R}}\left(\frac{I}{2\varepsilon_0 n_r c}\right)\frac{|\mu_{21}|^2\sigma_v\hbar\Gamma_0}{[(E_{21}-\hbar w)^2+(\hbar G_0)^2]^2}\left(4|m_{21}|^2 - \frac{\sigma_{12}^2[3E_{21}^2-4E_{21}\hbar w+\hbar^2(w^2-\Gamma_0^2)]}{E_{21}^2+(\hbar G_0)^2}\right) \quad , \quad (16)$$

where $\sigma_v$ is the density of electrons in the QWs, $E_{ij}=E_i-E_j$ is the energy interval of two different electronic states, $\mu_{ij}$ is the matrix element which is defined by $\mu_{ij}=|(\phi_i|ez|\phi_j)|$, $\sigma_{ij}=|\mu_{ii}-\mu_{ij}|(i,j=1,2)$, and I is the optical beam intensity. So the total absorption coefficient $\alpha(w,I)$ is given by

$$\alpha(w,I) = \alpha^{(1)}(w) + \alpha^{(3)}(w,I) \quad . \quad (17)$$

## 2 Numerical results and discussion

In order to see more clearly the dependent behaviors of linear and nonlinear optical absorptions on the structural parameters of the wurtzite step QWs, the numerical calculations were performed on an asymmetrical AlN/GaN/$Al_xGa_{1-x}N$/AlN step QW in the present section. The material parameters used in our calculations are listed in Table 1[3]. The other parameters used in our calculations are as follows: [3] $\sigma_v = 5\times10^{22}\ \mathrm{m}^{-3}$, $\varepsilon_R = 5.43\ \varepsilon_0$, $\Gamma_0^{-1} = 100$ fs

**Table 1　Material parameters for GaN, AlN, and $Al_xGa_{1-x}N$ [3]**
**表 1　GaN, AlN, 和 $Al_xGa_{1-x}N$ 的材料参数[3]**

| | | GaN | AlN | $Al_xGa_{1-x}N$ |
|---|---|---|---|---|
| Band gap (eV) | $E_g$ | 3.39 | 6.20 | $6.20x+3.39(1-x)-0.6x(1-x)$ |
| Lattice constant (Å) | $a$ | 3.189 | 3.11 | $3.11x+3.189(1-x)$ |
| | $c$ | 5.185 | 4.89 | $4.89x+5.185(1-x)$ |
| Piezoelectric constant ($C/m^2$) | $e_{31}$ | -0.49 | -0.60 | $-0.60x-0.49(1-x)$ |
| | $e_{33}$ | 0.73 | 1.46 | $1.46x+0.73(1-x)$ |
| Elastic constant (GPa) | $c_{31}$ | 103 | 108 | $103x+108(1-x)$ |
| | $c_{33}$ | 373 | 405 | $405x+373(1-x)$ |
| Effect mass | $m^{*}$ | 0.22 | 0.33 | $0.33x+0.22(1-x)$ |
| Static dielectric constant | $\varepsilon_0$ | 9.2 | 8.5 | $8.5x+9.2(1-x)$ |
| Electronic dielectric constant | $e_e$ | 5.35 | 4.77 | $4.89x+4.77(1-x)$ |
| Spontaneous polarization ($C/m^2$) | $P_{SP}$ | -0.029 | -0.081 | $-0.081x-0.029(1-x)$ |

Before analyzing the properties of optical absorption, it is necessary to discuss the electronic states and geometric factors in the wurtzite step QW with strong BEF. In Fig. 1, besides the material structures and potential profile, the ground-state electronic wavefunction $[\phi_1(z)]$ and the first excited wavefunction $\phi_2(z)$ in the step QW are depicted. And their energy levels correspond to $E_i(i=1,2)$. It is observed that the ground state $\phi_1(z)$ is mainly localized in the right side of the GaN well-region due to the effect of BEF, and the first excited state $\phi_2(z)$ distributes in the central $Al_xGa_{1-x}N$ barrier-region, which is beneficial to obtaining large geometric factors in the quantum structures.

In Fig. 2, the geometric factors $\mu_{12}$ (solid lines) and (dash lines) of the GaN-based step QWs as func-

tions of the well width $L_w$[Fig. 2 (a)], the central step barrier width $L_b$[Fig. 2 (b)] and the doped concentration $x$ of the step barrier [Fig. 2(c)] are plotted. The geometric factors reach to several tens angstroms, which is also beneficial to observing strong optical absorption effect. Moreover, the dependences of the geometric factors on the structural parameters behave complicated functional relationships. From Fig. 2 (a), it is seen clearly that both the geometric factors $\mu_{12}$ and $\sigma_{12}$ have maximum at certain well width. With the increase of the central barrier width, the geometric factor $\mu_{12}$ increases monotonically, while $\sigma_{12}$ decreases monotonically in Fig. 2 (b). It is observed that in Fig. 3(c) that the geometric factor $\mu_{12}(\sigma_{12})$ increases (decreases) monotonically as the doped concentration $x$ of the step barrier increases. The magnitude of geometric factors reveals the distribution and overlapping situations of the electronic wave-functions. In fact, the electronic wave-functions in the GaN-based step QWs are determined jointly by the confined potential, the BEF and the band nonparabolicity as well as many other factors. This directly results in the complicated dependence relationship of geometric factors on the structural parameters.

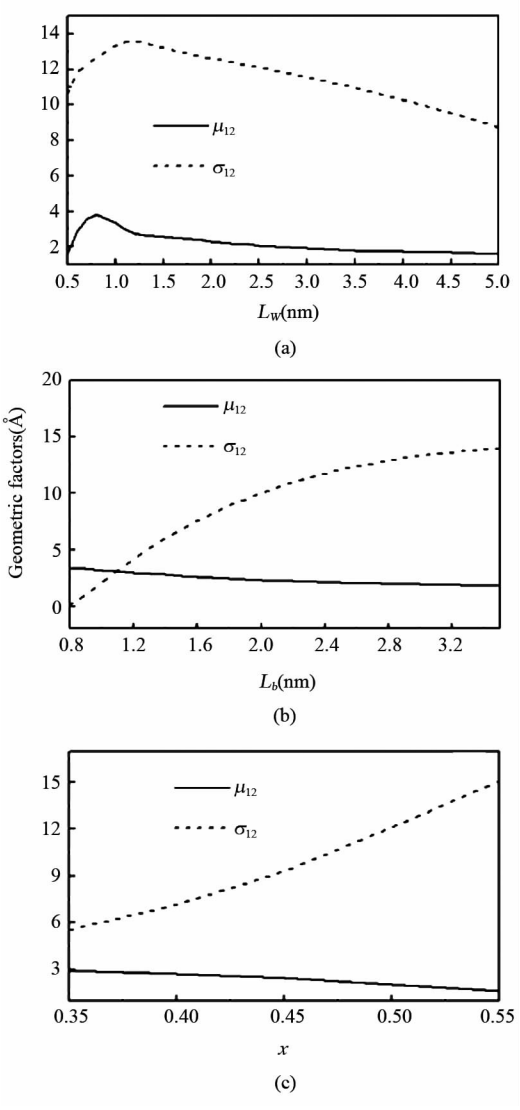


Fig. 2 Geometric factors $\mu_{12}$ (solid lines) and $\sigma_{12}$ (dash lines) of the GaN-based step QWs as functions of the well width $L_w$[Fig. 2 (a)], the central step barrier width $L_b$[Fig. 2 (b)] and the doped concentration $x$ of the step barrier [Fig. 2(c)]

图2 GaN-基阶梯量子阱中几何因子 $\mu_{12}$(实线)及 $\sigma_{12}$(虚线)随阱宽 $L_w$(图2a),中间阶梯垒宽 $L_b$(图2b)及阶梯垒的掺杂浓度 $x$(图2c)变化曲线

Figure 3 depicts the linear $|\alpha^{(1)}(w)|$ (solid lines), the nonlinear $|\alpha^{(3)}(w,I)|$ (dash lines) and the total absorption coefficients $\alpha(w,I)$ (dot lines) as a function of the incident photon energy $\hbar w$ when the optical beam intensity $I$ is fixed at $10\times10^{11}$ W/m$^2$. Three different structural parameters are chose. In Fig. 3 (a), the step barrier width is a variable parameter and the well width and doped concentration $x$ are kept at 2.5 nm and 0.5, respectively. In Fig. 3 (b), the well width is a variable parameter and the step barrier width and doped concentration $x$ are kept at 2.5 nm and 0.5, respectively. In Fig. 3 (c), the doped concentration $x$ is a variable parameter and both the well width and the step barrier width are kept at 2.5 nm. From Fig. 3(a), it is observed that the linear and nonlinear absorption coefficients reach about $10^4$ m$^{-1}$ and $10^3$ m$^{-1}$, respectively, which are consistent with the magnitude of experimental results in InN/InGaN multiple QWs.[5,8] With the increase of the central step AlGaN barrier, the energies of absorption photon have obvious red-shift due to the fact that the weaker quantum confined effect results in the lower transition energy $E_{12}$ between the ground state and the first excited state. For example, as $L_b$ decrease from 2.0 nm to 1.0 nm, the phonon energy shifts from 500 meV to 670 meV. If $L_b$ further decreases ($L_b<1$ nm), the energy of absorption photon will approach 800 meV, which corresponds to the optical telecommunication wavelengths ~1.55 μm.[6,8] With the decrease of $L_b$, the absorption coefficients $|\alpha^{(1)}(w)|$ and $|\alpha^{(3)}(w,I)|$ increase obviously, but the total absorption coefficients $\alpha(w,I)$ increase slightly, and the FWHM of $\alpha(w,I)$ increase. As $L_b=1.5$ nm, the total absorption coefficient in contrast to the linear one decreases about 50%, which means the saturation absorption intensity is about $I=10\times10^{11}$ W/m$^2$. And $\alpha(w,I)$ in contrast to $|\alpha^{(1)}(w)|$ decreases about 38.39% (73.08%) as $L_b=2.0$ nm (1.0 nm). This reveals that the saturation absorption intensity decrease with the decrease of the barrier width $L_b$.

From Fig. 3(b), it is seen clearly that the linear and nonlinear as well as the total absorption coefficients decrease with the increase of the well width $L_w$. Moreover, as $L_w$ decreases, the photon energies of absorption have obviously blue-shift, which is completely consistent with the experimental observation in GaN/AlGaN multiple QW structures[6]. The FWHM of the total absorption coefficient increases and the saturation absorption intensity decreases when the well width decreases.

From Fig. 3(c), it is found that, as the doped concentration $x$ of step barrier decrease from 0.45 to 0.35, the linear and nonlinear absorption coefficients increase significantly. And the photon energies of absorption also

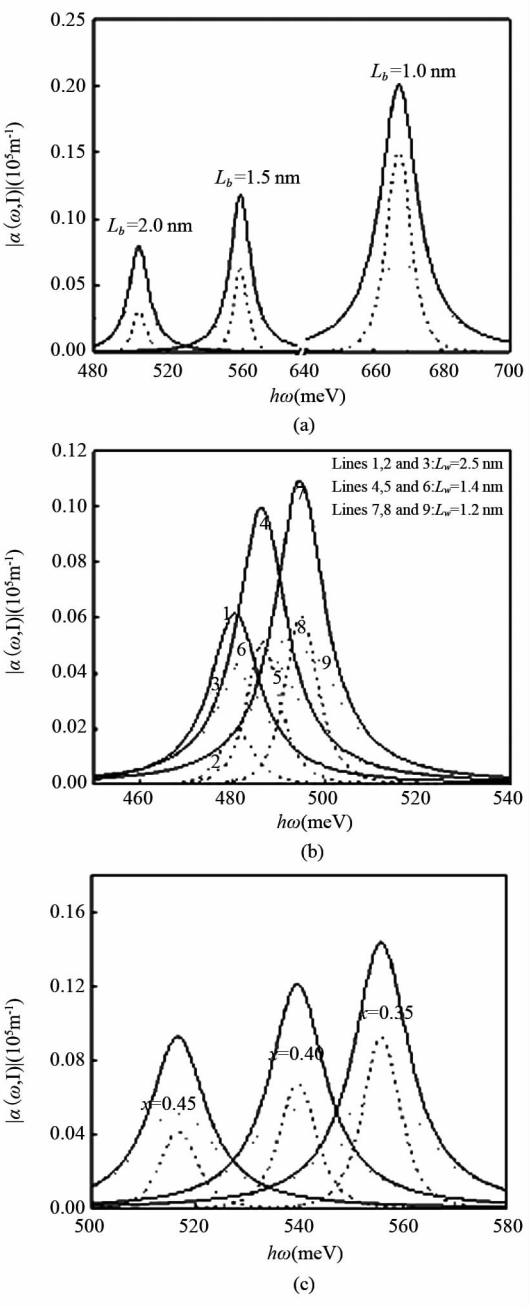


Fig. 3 Linear $|\alpha^{(1)}(w)|$ (solid lines), the nonlinear $|\alpha^{(3)}(w,I)|$ (dash lines) and the total absorption coefficients $\alpha(w,I)$ (dot lines) as a function of the incident photon energy $\hbar w$ when the optical beam intensity is fixed at $10 \times 10^{11}$ W/m$^2$. In Fig. (a), the well width and doped concentration $x$ are kept at 2.5 nm and 0.5, respectively. In Fig. (b), the step barrier width and doped concentration $x$ are kept at 2.5 nm and 0.5, respectively. In Fig. (c), both the well width and the step barrier width are kept at 2.5 nm

图 3 当光束强度固定在 $10 \times 10^{11}$ W/m$^2$. 时,线性吸收系数 $|\alpha^{(1)}(w)|$(实线), 非线性吸收系数 $|\alpha^{(3)}(w,I)|$(虚线)及总吸收系数 $\alpha,(w,I)$(点线)随入射光子能量 $\hbar w$ 变化曲线. 在图 3a 中, 阱宽与掺杂浓度分别固定在 2.5nm 及 0.5. 在图 3b 中,阶梯垒宽及掺杂浓度分别固定在 2.5nm 与 0.5. 在图 3c 中, 阱宽及阶梯垒宽均被固定在 2.5nm

behave obviously blue-shift. This observation is different from the case of GaN-based multiple QW systems[6]. In GaN-based multiple QW systems, the ISB absorption shows a systematic red shift for decreasing Al mole fraction in the barriers. The reason for this difference may be ascribed to the structural variation between the GaN-based step QW and multiple QW. Moreover as $x$ increases, the FWHM of the total absorption coefficient decreases, and the saturation absorption intensity obviously increases. Comparing Fig. 3(a), (b) and (c), it is found that, in contrast to the well width of GaN-based step QWs, the width and the doped concentration of the step barrier have important and obvious influences on the absorption coefficients. Therefore, in order to obtain optimizational absorption coefficients in GaN-based step QW, adjusting the barrier width and doped concentration of the step barrier are effective approach and choice.

## 3 Conclusion

In conclusion, by using the compact density matrix approach, the linear and nonlinear optical absorption coefficients in a four-layer GaN-based step QW with strong BEF have been theoretically deduced and investigated in detail. The band nonparabolicity is taken into account by using an EDEM method. The analytical electronic states were derived by the two Airy functions. Numerical calculations on an AlN/GaN/AlGaN/AlN step QW were performed, and the curves for the geometric factors, the linear, the nonlinear and the total optical absorption coefficients as functions of the structural parameters of the step QW are plotted. The features for these curves were specified and reasons for the features were explained reasonably. It is found that decreasing the well width $L_w$, step barrier width $L_b$, and the doped concentration x in step barrier will result in the enhancement of the absorption coefficients. Moreover, with the decrease of $L_w$, $L_b$ and $x$, the photon energies of absorption have blue-shift, and the FWHM of the total absorption coefficient increases and the saturation absorption intensity decreases. Some results obtained here agree with the recent experimental observations[6]. Therefore, theoretical study may make a great contribution to experimental studies. We hope that these theoretical results could invoke more experimental explore of optical absorption in nitride step QW structures.

## References

[1] LIZUKA N, KANEKO K, SUZUKI N. Near-infrared intersubband absorption in GaN/AlN quantum wells grown by molecular beam epitaxy [J]. *Appl. Phys.* Lett., 2002, **81**: 1803 - 1805.

[2] TCHERNYCHEVA M, NEVOU L, DOYENNETTE L, *et al*. Optical and theoretical study of strong electron coupling in double GaN/AlN quantum wells [J]. *Phys. Stat. Sol. B*, 2006, **243**: 1630 - 1633.

[3] SHI Jun-Jie, XIA Cong-Xin, WEI Shu-Yi, *et al*. Exciton states in wurtzite InGaN strained coupled quantum dots: Effects of piezoelectricity and spontaneous polarization [J]. *J. Appl. Phys.*, 2005, **97**: 083705 (1 - 8).

[4] LI Y, PAIELLA R. Intersubband all-optical switching based on Coulomb-induced optical nonlinearities in GaN/AlGaN coupled quantum wells [J]. *Semicond. Sci. Technol.*, 2006, **21**: 1105 - 1110.

[5] MALIS O, EDMUNDS C, MANFRA M J, *et al*. Near-infrared intersubband absorption in molecular-beam epitaxy-grown lattice-matched

InAlN/GaN superlattices[J]. *Appl. Phys. Lett*, 2009, **94**: 161111 (1-3).

[6] MONROY E, KANDASWAMY P K, MACHHADANI H, *et al*. Polar and Semipolar III-Nitrides for long wavelength intersubband devices, Proc. SPIE 7608, Quantum Sensing and Nanophotonic Devices VII [J], 2010, 76081G doi:10.1117/12.847027.

[7] HOFSTETTER D, DI FRANCESCO J, KANDASWAMY P K. Intersubband spectroscopy probing higher order interminiband transitions in AlN-GaN-based superlattices [J]. *Appl. Phys*. Lett., 2011, **98**: 071104 (1-3).

[8] NARANJO F B, KANDASWAMY P K, VALDUEZA-Felip S, *et al*. Nonlinear absorption of InN/InGaN multiple-quantum- well structures at optical telecommunication wavelengths [J]. *Appl. Phys*. Lett., 2011, **98**: 031902 (1-3).

[9] IVE T, BERLAND K, STATTIN M, *et al*. Design and Fabrication of Nitride Heterostructures for Intersubband Applications [J], *International Proceedings of Computer Science & Information Tech*., 2012, **32**: 62-66.

[10] ROSENCHER E, BOIS Ph. Model system for optical nonlinearities: Asymmetric quantum wells [J]. *Phys. Rev. B*, 1991, **44**: 11315-11327.

[11] YUH P F, WANG K L. Optical transitions in a step quantum well [J]. *J. Appl. Phys*, 1989, **65**: 4377-4381.

[12] WANG Guang-Hui, GUO Qi. Effect of spatial nonlocality on terahertz optical interaction with quantum wells [J]. *J. Appl. Phys*. 2009, **105**: 073515 (1-5).